Semiconductor Chromophores

International Edition: DOI: 10.1002/anie.201505988
German Edition: DOI: 10.1002/ange.201505988

Orange Zinc Germanate with Metallic Ge–Ge Bonds as a Chromophore-Like Center for Visible-Light-Driven Water Splitting

Ling Qian, Jian Fu Chen, Yu Hang Li, Long Wu, Hai Feng Wang, Ai Ping Chen, P. Hu, Li Rong Zheng, and Hua Gui Yang**

Abstract: *The efficiency of solar-energy-conversion devices depends on the absorption region and intensity of the photon collectors. Organic chromophores, which have been widely stabilized on inorganic semiconductors for light trapping, are limited by the interface between the chromophore and semiconductor. Herein we report a novel orange zinc germanate (Zn-Ge-O) with a chromophore-like structure, by which the absorption region can be dramatically expanded. Structural characterizations and theoretical calculations together reveal that the origin of visible-light response can be attributed to the unusual metallic Ge–Ge bonds which act in a similar way to organic chromophores. Benefiting from the enhanced light harvest, the orange Zn-Ge-O demonstrates superior capacity for solar-driven hydrogen production.*

As one of the most abundant and yet least collected sources of renewable energy, solar energy has attracted considerable interest. However, enhancing light absorption for solar-harvesting devices still remains a challenge.[1] Sensitizing semiconductors with dyes containing organic chromophores has been demonstrated to be a promising way to extend the working wavelength of the solar energy spectrum.[2] In this way, photogenerated electrons from the excited state of the chromophore can inject into the conduction band of semiconductor, greatly increasing the photon-to-electron yield under visible light.[3] However, this system requires strict bandgap alignment of the organic chromophores and semiconductors, and the interface between the chromophore and semiconductor will block fast charge transport, thus hindering the efficiency of multi-electron transfer catalysis.[4] This limitation could be overcome, in principle, by the means of a built-in chromophore inside the semiconductor. However, it's very hard to construct a chromophore-like structure by modifying the local structure at atomic level. Zinc germanate (Zn_2GeO_4) has recently attracted intense research interests because of its potential applications in catalysis,[5] photoluminescence,[6] and optoelectronics.[7] Unfortunately, the bandgap of Zn_2GeO_4 is too large (4.68 eV) to enable visible light harvesting.

Herein, for the first time, we prepared an orange zinc germanate (Zn-Ge-O) with a built-in inorganic chromophore-like structure, which shows a dramatically expanded visible-light absorption range and narrowed bandgap (Scheme 1). Through combination of state-of-the-art X-ray absorption spectroscopy and theoretical calculations, we demonstrate that the origin of the visible light response can be attributed to the unusual metallic Ge–Ge bonds which act as the chromophore-like structure in the semiconductor. The concept of a built-in chromophore-like structure creates new ways and theoretic bases for enhancing the visible-light absorption of other semiconductors.

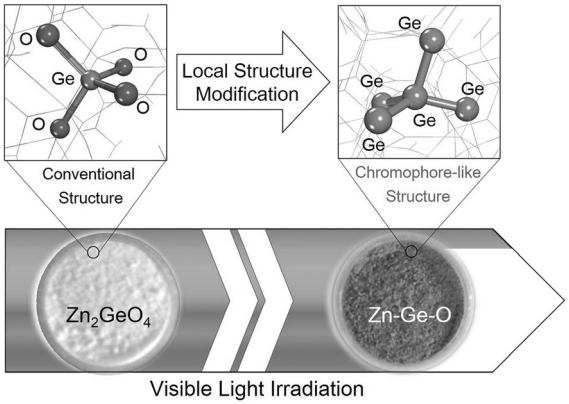

Scheme 1. Representative structural sections of the white Zn_2GeO_4 and orange Zn-Ge-O as deduced from experimental analyses and theoretical calculations. Left: a single Ge atom binding to four O atoms (conventional structure). Right: Ge cluster with Ge–Ge bonds for visible-light-absorption (chromophore-like structure).

The orange Zn-Ge-O was synthesized by a co-precipitation method, and the conventional white Zn_2GeO_4 was also prepared for comparison. In the UV/Vis absorption spectra,

[*] L. Qian,[+] Y. H. Li, Dr. L. Wu, Prof. A. P. Chen, Prof. H. G. Yang
Key Laboratory for Ultrafine Materials of Ministry of Education, School of Materials Science and Engineering, East China University of Science and Technology
130 Meilong Road, Shanghai, 200237 (China)
E-mail: hgyang@ecust.edu.cn
J. F. Chen,[+] Dr. H. F. Wang, Prof. P. Hu
Key Laboratory for Advanced Materials, Centre for Computational Chemistry and Research Institute of Industrial Catalysis, East China University of Science and Technology
130 Meilong Road, Shanghai, 200237 (China)
Prof. P. Hu
School of Chemistry and Chemical Engineering
the Queen's University of Belfast, Belfast BT9 5AG, UK
Dr. L. R. Zheng
Beijing Synchrotron Radiation Facility, Institute of High Energy Physics, Chinese Academy of Sciences
Beijing 100049 (China)
E-mail: zhenglr@ihep.ac.cn
[+] These authors contributed equally to this work.

Supporting information for this article is available on the WWW under http://dx.doi.org/10.1002/anie.201505988.

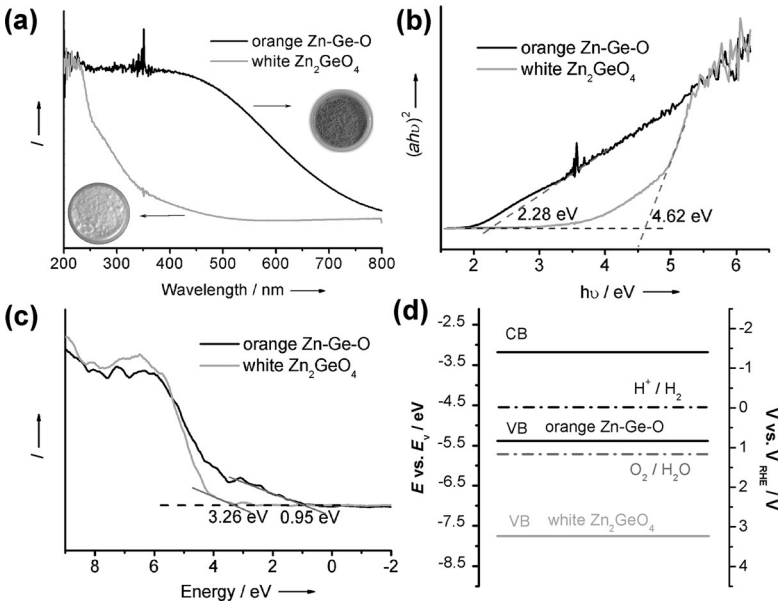

Figure 1. a) UV/Vis spectra, b) Tauc plots, c) valance-band XPS spectra, and d) band-structure diagram of white Zn_2GeO_4 and orange Zn-Ge-O.

the orange Zn-Ge-O exhibits an additional intense visible-light-absorption band (Figure 1a). Based on the Tauc plot ($(\alpha h\nu)^2$ versus $h\nu$), the orange Zn-Ge-O corresponds to a direct bandgap material and its bandgap (E_g) is approximately 2.28 eV while that of white Zn_2GeO_4 is approximately 4.62 eV (Figure 1b). The density of states (DOS) for the valance band of orange Zn-Ge-O and white Zn_2GeO_4 were also measured by valance-band X-ray photoelectron spectroscopy (XPS) (Figure 1c). The valance-band maximum energy of orange Zn-Ge-O is 0.95 eV, while that of the white Zn_2GeO_4 is 3.26 eV. Combined with optical measurements, the bandgap structure for both orange and white samples can be shown (Figure 1d), the conduction band (CB) of orange Zn-Ge-O shows no substantial change compared with white Zn_2GeO_4. The different atomic arrangement between the orange Zn-Ge-O and white Zn_2GeO_4 can be confirmed by the analysis of X-ray diffraction pattern (XRD) (Figure S1 in the Supporting Information), Raman spectra (Figure S2), transmission electron microscopy (TEM), and selected-area electron diffraction (SAED) image (Figure S3), energy-dispersive X-ray spectroscopy (EDX) (Figure S4), and XPS spectra (Figure S5).

To further investigate the local structure of orange Zn-Ge-O, X-ray absorption fine structure (XAFS) measurements were utilized, and XAFS spectra of Zn, ZnO, GeO_2, Ge, and white Zn_2GeO_4 were also measured as references. In Figure 2a, the peak at 1.0–2.0 Å in GeO_2 can be attributed to the scattering from the nearest oxygen atoms, and the peak at 2.0–3.0 Å in Ge powder corresponds to scattering from the neighboring Ge atoms. Thus, the peak at 2.0–3.0 Å of orange Zn-Ge-O is similar to that of Ge powder but different from that of white Zn_2GeO_4, suggesting the existence of Ge–metal bonds in orange Zn-Ge-O. Moreover, the presence of Ge–O is confirmed by the peaks at 1.0–2.0 Å for both the orange and white samples. In addition, the Zn K-edge spectra (Figure S6) of the white and orange samples exhibit little difference, indicating the similar local structural configuration of Zn binding. As the Zn binding structure is not clearly changed, the possibility of Ge–Zn binding can be safely ruled out. Simulation of the Ge K-edge spectra was performed. For the orange Zn-Ge-O, there is a Ge–O contribution at a distance of 1.76 Å with coordination number of 3.3, and the Ge–Ge distance is 2.47 Å with a coordination number of 1.7. The Ge–O and Ge–Ge distances in the orange Zn-Ge-O are in accord with reference values of GeO_2 and Ge powder.[8] Nevertheless, the coordination number of Ge–O (3.3) and Ge–Ge (1.7) are both less than those of GeO_2 and Ge (Table S1), suggesting that Ge species in the orange Zn-Ge-O contain mixed-valent Ge states. Figure 2b shows the normalized X-ray absorption near-edge structure spectra of the orange Zn-Ge-O and the reference samples. The intensities of the so-called white-line in the spectra reflect the oxidation state of Ge in different samples.[9] Therefore, the intensity of white Zn_2GeO_4 is a little higher than that of orange Zn-Ge-O, which implies the average oxidation state of Ge in the orange sample can be lower than Ge^{IV} in the white Zn_2GeO_4. According to the above structure analyses, the existence of Ge–Ge bonds causes a distinct structural rearrangement in the orange Zn-Ge-O, which can be the origin of its visible-light response.

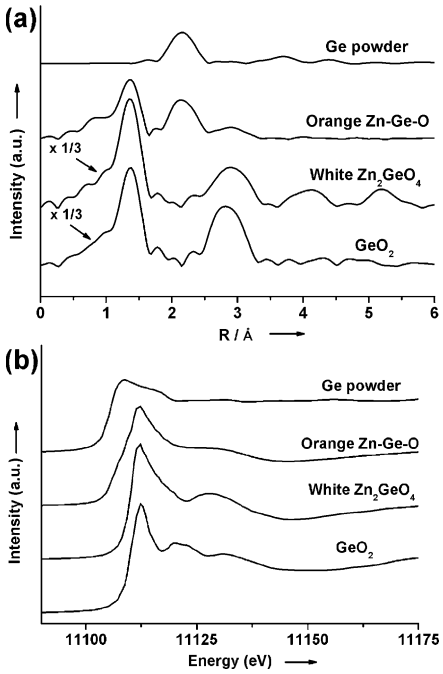

Figure 2. a) The k^3-weighted Fourier-transformed EXAFS spectra of Ge K-edge spectra, and b) normalized X-ray absorption near-edge structure spectra of Ge K-edge spectra of orange Zn-Ge-O and the reference samples.

To elucidate the origin of the enhancement of visible-light harvesting by orange Zn-Ge-O, a systematic electronic-structure analysis was performed by virtue of the state-of-the-art density-functional theory (DFT) calculations. Considering the crucial structural features of the amorphous Zn-Ge-O elucidated from the various experimental characterizations and theoretical information, several approaches, such as introducing an oxygen vacancy, Zn vacancy, or additional Ge by lattice substitution in the crystalline Zn_2GeO_4 were examined to determine the crucial features (see details in Supporting Information). The electronic structure of Zn_2GeO_4 was investigated as a reference. Zn_2GeO_4 crystalizes in the willemite structure, consisting of a series of GeO_4 and ZnO_4 tetrahedrons linked with by vertex-sharing at three-coordinated oxygen atoms, which are arranged to form a large- and small-sized pore along the [001] direction (Figure 3 a). Each oxygen atom is bound by one Ge and two Zn atoms to form a planar configuration. On the whole, these oxygen atoms can be classified into three types, containing the one as the corner atom shared by three small pores along the [001] direction (denoted as A), and the two other oxygen atoms types are at the large-pore wall with the difference being they face outward towards the nearest Zn or Ge (denoted as B and C), respectively. From the projected density of states (PDOS) of Zn_2GeO_4 shown in Figure 3 e, it can be found that the valence band maximum of Zn_2GeO_4 is mainly composed of the O-2p orbital and also some hybridization from the Zn-3d and Ge-4p orbital, while the conduction band minimum mainly consists of the Ge-4s and Ge-4p orbital. The bandgap of Zn_2GeO_4 is estimated to be 2.26 eV, which is similar with the previous theoretical work (2.0–2.1 eV).[10]

We examined the tuning effect of an O vacancy on the electronic structure. All the three possible kinds of O vacancies were checked, showing that the vacancy formed at the site A (denoted A0) is slightly more stable by approximately 0.1 eV compared with sites B and C, and thus was focused on. Accompanying the O vacancy formation, these two excess electrons are mainly localized at the 4p orbital of the nearest Ge atom (with a gain of approximately 1.3 *e* from the Bader charge), and correspondingly, a new occupied state appears near the Fermi level (Figure 3 f) and results in a slight narrowing of the bandgap to 2.0 eV. However, the resultant structure after removing O does not fully reflect the key structural feature in experiment; the distance between Ge and Zn atom or Ge and Ge atom near the O vacancy is still too long to bond directly and hardly form Ge-rich center. To construct a local Ge-rich center, a feasible approach upon careful examination is to introduce external Ge atoms in the Zn_2GeO_4 framework containing O vacancies. After full optimization, the introduced Ge atom prefers to refill the O vacancy and relax outward from the initial O_{3c} plane owing to the steric strain. As a result, it would form a distorted tetrahedral configuration with one Ge–Ge bond, two Ge–Zn bonds and one Ge–M bond, in which M is O, Zn, or Ge, corresponding to the case of substituting O at the site A, B, or

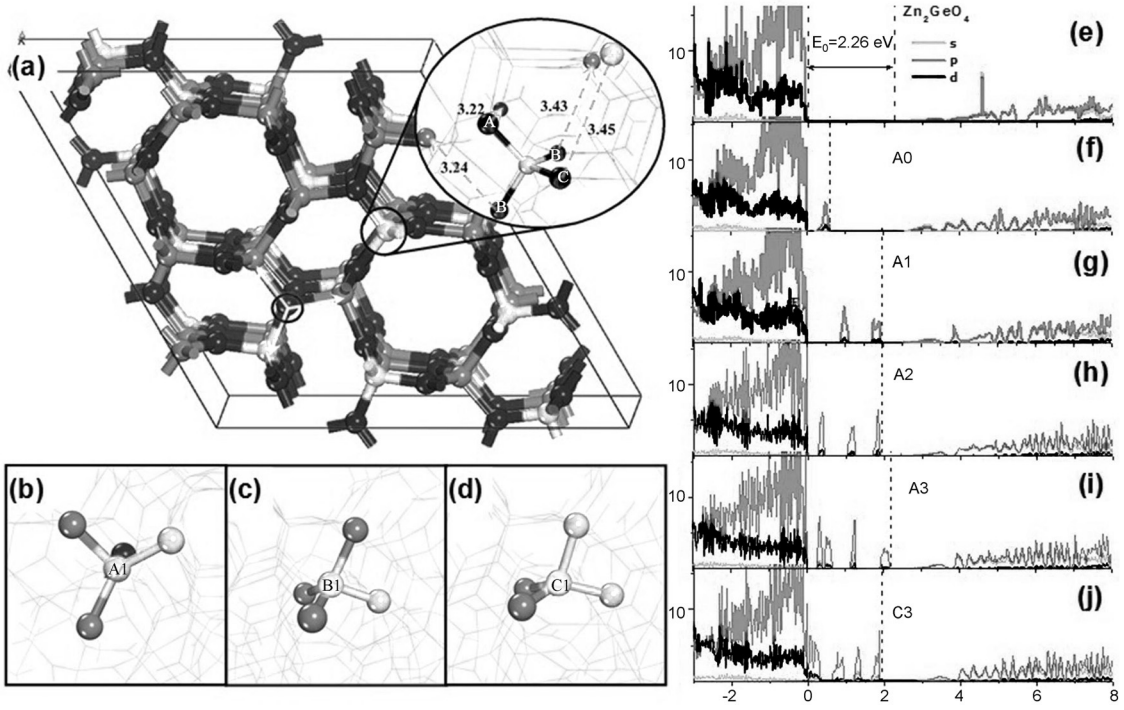

Figure 3. a) Ball-and-stick model of the optimized unit cell for the bulk Zn_2GeO_4. Inset: the magnified coordination environment of the lattice O atom. White balls represent Ge, gray for Zn, and black for O. This color code is used throughout this work. b)–d) illustrate the possible coordination environment of the central Ge atom in the Ge-rich tetrahedrons, in which (b) indicates configuration A1, (c) B1, and (d) C1. e)–j) give the corresponding projected density of states (PDOS) of the amorphous Zn-Ge-O compound (denoted as $Zn_{2-x}Ge_{1+x+y}O_{4-y}$) with different kinds of Ge-rich center, in which the PDOS of bulk Zn_2GeO_4 (e) is also given as a benchmark. To better uncover the origin of the bandgap variation, all the energy levels are aligned to the 1s orbital of the lattice O in the intact Zn_2GeO_4 framework. For details see text.

C with Ge, respectively. As shown in Figure 3 b–d, the three tetrahedral configurations can be denoted as A1, B1 and C1. DFT results indicate that the A1 configuration is much more stable than B1 and C1 by about 1 eV, therefore, it should exist in majority. Herein we would focus on the A1 configuration, despite that the configuration B1 and C1 are also tested to give a similar trend (see details in Figures S7, S8).

In the A1 configuration, the central Ge atom forms one Ge–Ge bond, two Ge–Zn bonds, and one Ge–O bond, and the corresponding bond lengths are calculated to be 2.38 Å, 2.32 Å, and 2.10 Å. Bader charge analysis indicates that the central Ge atom is reduced with a weak positive charge ($+0.18\,e$) compared with the original Zn_2GeO_4 ($+2.15\,e$). As seen from the density of state in Figure 3 g, there are two evident occupied gap states mainly attributed to the reduced Ge atom, which narrow the bandgap for the electronic excitation to about 0.5 eV. Furthermore, we examined the possible Ge-rich configuration with more Ge–Ge bonds by substituting the Zn atom with Ge, corresponding to configuration A2 and A3, in which one and two Zn atoms are substituted, respectively. With the increase of the number of Ge–Ge bonds, it indicates the central Ge atom becoming more negatively charged. For example, with respect to the configuration A3 with three Ge–Ge bonds and one Ge–Zn bond, the central Ge atom has $+0.03\,e$. In addition, the average Ge–Ge bond length from A1 to A3 increases from 2.38 to 2.42 Å, being closer to the experimental value (2.47 Å, Table S1). As seen in Figure 3 g–i, the DOS indicates that more gap states appear relative to the A1 configuration, and importantly, all the bandgaps were evidently narrowed. Specifically, by comparing the DOS shown in Figure 3 g–i, it can be seen that all the emerging gap states are mainly attributed to the reduced Ge-4p orbital, and the number of gap states has a linear correlation with the number of Ge–Ge bonds in the Ge-rich tetrahedron. Interestingly, we also consider a stable configuration C3 comparable with A3, corresponding to a highly reduced Ge-rich tetrahedron with four Ge–Ge bonds (Figure S7g). The Bader charge of the central Ge is calculated to be $-0.08\,e$, and the average Ge–Ge bond length is 2.42 Å, indicating that the C3 configuration matches well with experimental XPS (Ge^0) and EXAFS result. The electronic structure analysis indicates that its bandgap is also notably reduced to approximately 1.0 eV.

One of the most interesting properties of semiconductors where charge carriers can be created by irradiation is photocatalysis of reactions, such as water splitting, in which many exciting breakthroughs have been made to efficiently utilize the visible light accounting for 43% of the solar energy.[11] As illustrated in Figure 4, after loading of 1 wt% Pt as co-catalyst, the orange Zn-Ge-O displayed a continuous H_2 production ability of 26.9 $\mu mol\,h^{-1}$ under ultraviolet-visible light and 11.5 $\mu mol\,h^{-1}$ under visible light, whereas the white Zn_2GeO_4 with and without Pt loading showed negligible activity. The generation rate of orange Zn-Ge-O without Pt loading is 2.6 $\mu mol\,h^{-1}$ under visible light. To exclude the generation of H_2 from the residual sodium borohydride, the hydrogen evolution experiments were repeated under dark using Zn-Ge-O/Pt (1.0 wt%) and Zn-Ge-O as photocatalyst. No hydrogen is generated in both cases, indicating that the generation of hydrogen is from the photocatalytic reaction not from residual sodium borohydride. We also determined the photocatalytic activity with different content of Ge (Table S3), and the sample with the best performance can be the Zn-Ge-O photocatalyst with Ge/Zn ratio of about 1 (Figure S9). The photocatalytic performance of Zn-Ge-O shows a sign of decay, therefore, with the loading of Pt and addition of methanol, both of the rate of H_2 evolution and stability can be enhanced (Figure S10). During the three cycles, H_2 can be produced constantly at a rate of around 14.1 $\mu mol\,h^{-1}$, and the performance decays only 7.96% after 72 h. The above results significantly suggest that the orange Zn-Ge-O is photoreactive under visible light irradiation.

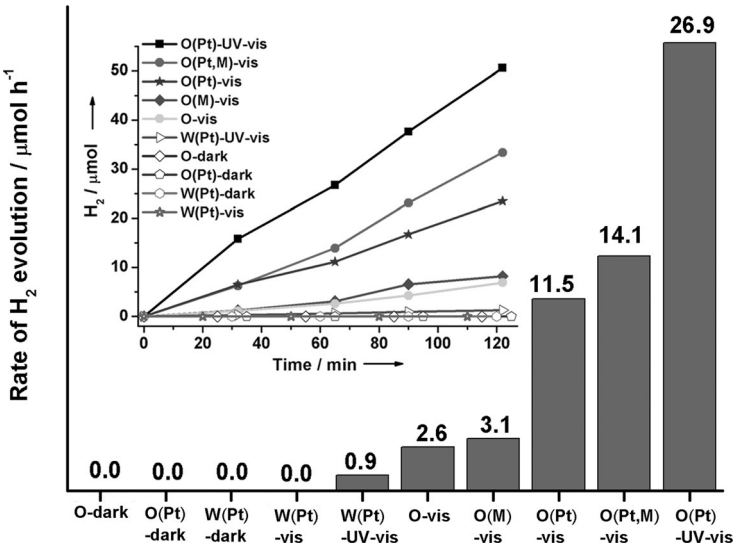

Figure 4. H_2 evolution rate of orange Zn-Ge-O and white Zn_2GeO_4 under different conditions. Inset: The reaction time profile of hydrogen evolution. (O = orange Zn-Ge-O; W = white Zn_2GeO_4; M = methanol; vis = visible light; UV-vis = ultraviolet–visible light).

In summary, we report an unexpected orange Zn-Ge-O semiconductor with enhanced photocatalytic hydrogen evolution performance under visible light irradiation. Through comprehensive characterizations, in-depth analysis, and first-principle calculations, we find that the Ge–Ge bonds formed in the orange Zn-Ge-O can act as a light-absorbing chromophore-like structure, which plays a crucial role in enhancing the visible-light adsorption. We believe that this new kind of built-in chromophore-like structure in semiconductors could be expanded to other materials for efficient solar light utilization.

Acknowledgements

This work was financially supported by National Natural Science Foundation of China (21373083), Program of Shanghai Subject Chief Scientist (15XD1501300) and Science and

Technology Commission of Shanghai Municipality (14JC1490900).

Keywords: chromophore-like structures · Ge—Ge bonds · hydrogen evolution · semiconductors · visible-light responsive

How to cite: *Angew. Chem. Int. Ed.* **2015**, *54*, 11467 – 11471
Angew. Chem. **2015**, *127*, 11629 – 11633

[1] a) N. S. Lewis, D. G. Nocera, *Proc. Natl. Acad. Sci. USA* **2006**, *103*, 15729 – 15735; b) H. B. Gray, *Nat. Chem.* **2009**, *1*, 7.
[2] a) P. Poddutoori, D. T. Co, A. P. S. Samuel, C. H. Kim, M. T. Vagnini, M. R. Wasielewski, *Energy Environ. Sci.* **2011**, *4*, 2441 – 2450; b) B. S. Veldkamp, W. S. Han, S. M. Dyar, S. W. Eaton, M. A. Ratner, M. R. Wasielewski, *Energy Environ. Sci.* **2013**, *6*, 1917 – 1928.
[3] O. V. Prezhdo, W. R. Duncan, V. V. Prezhdo, *Acc. Chem. Res.* **2008**, *41*, 339 – 348.
[4] Q. Liu, Y. Zhou, J. Kou, X. Chen, Z. Tian, J. Gao, S. Yan, Z. Zou, *J. Am. Chem. Soc.* **2010**, *132*, 14385 – 14387.
[5] Z. Liu, X. Jing, L. Wang, *J. Electrochem. Soc.* **2007**, *154*, 500 – 506.
[6] C. Yan, N. Singh, P. S. Lee, *Appl. Phys. Lett.* **2010**, *96*, 053108.
[7] Y. Jin, Y. Hu, Y. Fu, Z. Mu, G. Ju, *Mater. Lett.* **2014**, *134*, 187 – 189.
[8] a) O. Ohtaka, A. Yoshiasa, H. Fukui, K. Murai, M. Okube, H. Takebe, Y. Katayama, W. Utsumi, *J. Phys. Condens. Matter* **2002**, *14*, 10521 – 10524; b) G. Dalba, P. Fornasini, M. Grazioli, F. Rocca, *Phys. Rev. B* **1995**, *52*, 11034 – 11043.
[9] Y. H. Li, J. Xing, J. Chen, Z. Li, F. Tian, L. Zheng, H. F. Wang, P. Hu, H. Zhao, H. G. Yang, *Nat. Commun.* **2013**, *4*, 2500.
[10] a) J. Sato, H. Kobayashi, K. Ikarashi, N. Saito, H. Nishiyama, Y. Inoue, *J. Phys. Chem. B* **2004**, *108*, 4369 – 4375; b) Q. Liu, Y. Zhou, Z. Tian, X. Chen, J. Gao, Z. Zou, *J. Mater. Chem.* **2012**, *22*, 2033 – 2038; c) I. k. Oh, M. K. Kim, J. S. Lee, C. W. Lee, C. Lansalot-Matras, W. Noh, J. Park, A. Noori, D. Thompson, S. Chu, W. J. Maeng, H. Kim, *Appl. Surf. Sci.* **2013**, *287*, 349 – 354; d) R. A. Evarestov, A. V. Bandura, *J. Comput. Chem.* **2012**, *33*, 1123 – 1130.
[11] a) J. Liu, Y. Liu, N. Y. Liu, X. Zhang, H. Huang, Y. Lifshitz, S. T. Lee, J. Zhong, Z. H. Kang, *Science* **2015**, *347*, 970 – 974; M. G. Kibria, F. A. Chowdhury, S. Zhao, B. ALOtaibi, M. L. Trudeau, H. Guo, Z. Mi, *Nat. Commun.* **2015**, *6*, 6797; L. D. Li, J. Q. Yan, T. Wang, Z. J. Zhao, J. Zhang, J. L. Gong, N. J. Guan, *Nat. Commun.* **2015**, *6*, 5881; W. Y. Wang, J. Chen, C. Li, W. M. Tian, *Nat. Commun.* **2015**, *5*, 4647; C. S. Pan, T. Takata, M. Nakabayashi, T. Matsumoto, N. Shibata, Y. Ikuhara, K. Domen, *Angew. Chem. Int. Ed.* **2015**, *54*, 2955 – 2959; *Angew. Chem.* **2015**, *127*, 2998 – 3002; S. Chen, Y. Qi, T. Hisatomi, Q. Ding, T. Asai, Z. Li, S. S. Khine Ma, F. X. Zhang, K. Domen, C. Li, *Angew. Chem. Int. Ed.* **2015**, *54*, 8498 – 8501; *Angew. Chem.* **2015**, *127*, 8618 – 8621; R. S. Sprick, J. X. Jiang, B. Bonillo, S. J. Ren, T. Ratvijitvech, P. Guiglion, M. A. Zwijnenburg, D. J. Adams, A. I. Cooper, *J. Am. Chem. Soc.* **2015**, *137*, 3265 – 3270.

Received: June 30, 2015
Published online: August 20, 2015

